Supplement of Geosci. Model Dev., 8, 2857–2876, 2015
http://www.geosci-model-dev.net/8/2857/2015/
doi:10.5194/gmd-8-2857-2015-supplement

Geoscientific Model Development
Open Access

Supplement of

GNAQPMS-Hg v1.0, a global nested atmospheric mercury transport model: model description, evaluation and application to trans-boundary transport of Chinese anthropogenic emissions

H. S. Chen et al.

Correspondence to: Z. F. Wang (zifawang@mail.iap.ac.cn)

S1 Mercury chemistry

S1.1 Bromine oxidation

As shown in Table S1, we add five Br chemical reactions in the gas phase (Seigneur and Lohman, 2008) in addition to the O_3-OH oxidation mechanism to test how the Br oxidation reactions affect the Hg distributions. Similar to the treatment of Holmes et al. (2006, 2010), the five reactions are treated as a single reaction, with an effective Hg(0) first-order rate constant that is a function of the individual reaction rates and the concentrations of Br, BrO and OH based on the assumption that Br, BrO and OH concentrations don't change by their reactions with Hg. This is also the same with the implementation described in CAMx (2014). The effective first-order rate constant is calculated as follows:

$$k_{eff} = \frac{k_1[Br](k_3[Br]+k_4[OH])}{k_2+k_3[Br]+k_4[OH]} + k_5[BrO] \quad s^{-1}$$

In the GNAQPMS-Hg model, Br and BrO are not explicitly simulated. Therefore, we specify typical vertical profiles of Br and BrO concentrations over land and ocean, with higher values over ocean (2.9×10^{-8} and 2.9×10^{-7} ppm for Br and BrO) than over land (5.0×10^{-9} and 5.0×10^{-8} ppm for Br and BrO). During the night, the concentrations of Br and BrO are assumed to be zero, considering that the photolysis of Br_2 is the primary source for these radicals.

S1.2 Gas-particle partitioning of Hg(II)

The mechanism of gas-particle partitioning of Hg(II) implemented in GNAQPMS-Hg is based on the studies of Rutter and Schauer (2007a, b). Similar mechanisms are also used by the CAMx model and Vijayaraghvan et al. (2008). Rutter and Schauer (2007a) suggest that surface area rather than particulate matter (PM) mass controls the Hg(II) partitioning process. The surface-area adsorption coefficient (K_{sa}) is calculated as follows:

$$K_{sa} = Hg_{p,ads}/(RGM \times A_{sp} \times PM)$$

where K_{sa} is in $m^3\,m^{-2}$, $Hg_{p,ads}$ and RGM are in pg m^{-3}, A_{sp} is the specific surface

area of PM in m^2 μg^{-1} and PM is the ambient urban PM concentration in μg m^{-3}. Further, they also found that the K_{sa} obtained for urban PM falls between that of ammonium sulfate and adipic acid and it can be expressed as a function of temperature (K):

$$K_{sa} = 10^{\left(\frac{4250}{T}-10\right)}$$

Besides, studies also found a ten-fold increase in adsorption of RGM to sodium chloride compared to ammonium sulfate and organic particulate compounds. Therefore, K_{sa} for sea-salt is about 10 times that for urban PM:

$$K_{sa} = 10^{\left(\frac{4250}{T}-9\right)}$$

For simplicity, we treat all non-sea-salt PM as urban PM and use the above two equations to simulate RGM adsorption to urban PM and sea-salt PM, respectively. Therefore, the effective adsorption coefficient for each aerosol size section is calculated as follows:

$$K_{sa,eff} = 10^{\left(\frac{4250}{T}-9\right)} \times F_{ss} + 10^{\left(\frac{4250}{T}-10\right)} \times (1 - F_{ss})$$

where is F_{ss} the fraction of sea-salt in that size section.

S2 Mercury deposition

S2.1 Dry deposition

In the model, dry deposition is treated as a first-order removal mechanism. The deposition flux of a pollutant to the surface is the product of a characteristic deposition velocity and its concentration in the surface layer. Deposition velocities are derived from models that account for the reactivity, solubility, and diffusivity of gases, the sizes of particles, local meteorological conditions, and season-dependent surface characteristics. Dry deposition parameterizations of gases and aerosols are based on the work of Wesely (1989) and Slinn and Slinn (1980), respectively.

For gases, deposition velocity V_d is calculated from three primary resistances r (s m^{-1})in series as described below.

$$V_d = \frac{1}{r_a + r_b + r_s}$$

The aerodynamic resistance r_a represents bulk transport through the lowest model layer by turbulent diffusion. The quasi-laminar sub-layer resistance r_b represents molecular diffusion through the thin layer of air directly in contact with the particular surface to which material is being deposited. The surface resistance r_c depends upon the physical and chemical properties of the surface.

For particles, surface deposition occurs via diffusion, impaction, and gravitational settling. Particle size is the dominant variable controlling these processes. Particle deposition velocity for a given aerosol size is calculated using the following resistance equation.

$$V_d = V_{sed} + \frac{1}{r_a + r_b + r_a r_b v_{sed}}$$

V_{sed} is the gravitational settling (or sedimentation) velocity which is dependent on aerosol size and density.

The detail formulations of how to calculate r_a, r_b, r_s and V_{sed} for gases and aerosols can be found in Wesely (1989) and Slinn and Slinn (1980) or the user's guide of the CAMx model (CAMx, 2014).

In the GNAQPMS-Hg model, dry deposition of Hg(0), Hg(II) and Hg(P) are all accounted for by adaption the parameterizations described above. Several physical properties (e.g. Henry's law constant, molecular weight, surface reactivity) of the Hg species are specified in order to calculate their deposition velocities. The Henry's Law constant for Hg(0) is set to be 0.11 M atm^{-1} (Lin and Pehkonen, 1999) with a temperature factor of -4970 K (Clever et al., 1985), and the surface reactivity is set to zero. Hg(II) represents $HgCl_2$ and $Hg(OH)_2$. Its Henry's Law constant is assumed to be the same as HNO_3 because they have similar solubility (Bullock and Brehme, 2002). Like HNO_3, Hg(II) has a strong tendency to stick to surfaces and its dry deposition occurs readily, so the surface resistance for Hg(II) in the dry deposition scheme is set to zero. The Hg(P) dry deposition velocity is set equal to that for sulfate, similar to that applied in the CMAQ-Hg and STEM-Hg model (Bullock and Brehme, 2002; Pan et al., 2008).

S2.2 Wet deposition

In the model, wet deposition of the chemical species are calculated using an approach with medium complexity. In-cloud and below-cloud scavenging are included. The basic formulation implemented in the model is a scavenging approach in which the local rate of concentration change $\frac{\partial c}{\partial t}$ within or below a precipitating cloud depends on a scavenging coefficient Λ:

$$\frac{\partial c}{\partial t} = -\Lambda c$$

The scavenging coefficient is estimated differently for gases and particles, based on relationships described by Seinfeld and Pandis (1998). For gases, two components are calculated: 1) direct diffusive uptake of ambient gases into falling precipitation; and 2) accretion of cloud droplets that contain dissolved gases. For particles, there are also two components: 1) impaction of ambient particles into falling precipitation with an efficiency that is dependent upon particle size; and(2) accretion of cloud droplets that contain particle mass. Overall, the scavenging coefficient depends on an assumed scavenging efficiency, the total rainfall intensity (large-scale and convective precipitation), cloud water content and species solubility according to Henry's law, a mean cloud or rain droplet radius and rain droplet falling velocity. The large-scale and convective precipitation are not distinguished in this method. For species with low solubility (with a Henry's law constant of less than 100 M atm^{-1}), no wet deposition is calculated. More detail description of how to calculate the scavenging coefficients for gases and particles can be found in Seinfeld and Pandis (1998) or the user's guide of the CAMx model (CAMx, 2014). The physical properties (e.g. Henry's Law constant, surface reactivity, molecular diffusivity) of Hg species used in the wet deposition module are the same as those in the dry deposition module.

S3 Mercury emissions

The AMAP 2000 anthropogenic emission inventory was used in the model simulation. However, the emissions over South Africa in this inventory were reported to be flawed (AMAP/UNEP, 2008). Here, we assessed the effects of these flawed

emissions on the simulated results. As shown by Figure S7, we replaced the anthropogenic Hg emissions in South Africa by using the AMAP 2010 inventory and assessed this emission update on the simulated results. The emission amounts in South Africa decrease by about a factor of 4 (from 259 Mg to 64 Mg). After updating the emissions, the surface Hg concentrations in South Africa decrease by up to 1 ng m^{-3}, but have little changes elsewhere (the differences of concentrations are smaller than 0.01 ng m^{-3} in most areas) as shown by Figure S8. The simulated TGM concentrations at Cape Point decrease from 1.77 ng m^{-3} to 1.23 ng m^{-3}, more close to the observed values.

S4 Model evaluation

S4.1 Observational data

Due to limited public Hg observations, some model results were compared to observations with mismatched time periods. Actually, observations of wet deposition and precipitation in Europe and North America are from EMEP and MDN respectively, and the time periods are exactly the same with the simulation results. In contrast, no public Hg observation datasets are available in East Asia. So we used observations (collected from literatures) with mismatched time periods in East Asia.

All observations of Hg concentrations at land sites used in this study are averaged over time periods larger than 1 year. Analyses of long-term measurements show that trends in mean TGM during the last decade are small (of order $1\%a^{-1}$) or negligible at most background sites in the Northern Hemisphere (Temme et al., 2007; Wangberg et al., 2007). Therefore, the influences of the mismatch of time periods between model results and Hg concentration observations would not be large. Similar observational datasets (as shown in Table S2-S4) are also used by previous modeling studies (Selin et al., 2007, 2008; Holmes et al., 2010).

Observations from ship cruises are just used for initial comparison of simulated results over ocean following previous studies (Selin et al., 2007, 2008; Holmes et al., 2010). These observations are not used for quantitative model evaluation and not

including in the calculation of statistical parameters of model performance.

Annual dry and wet deposition measurements in East Asia (Table S5) are all obtained from literatures. Considering that dry and wet deposition fluxes are affected by environmental factors (e.g. precipitation) and they might differ from one year to another, so the influence of the mismatched time periods would be relatively larger. Again, no observations of Hg deposition are available at present. So there are no better choice.

Overall, the influence of the mismatch of the time periods between model results and observations is relatively large for dry and wet deposition comparisons in East Asia but relatively small for other comparisons. Quantitative assessments of the influence are difficult and outside the scope of this study.

S4.2 Diurnal and vertical variation

Fig. S12 compares the simulated and observed mean diurnal variations of TGM in St. Anicet, Delta, Mace Head, and Zeppelin. Detailed description of the observational sites can be found in Table S2. In St. Anicet, Mace Head, and Zeppelin, the TGM concentrations change little between daytime and nighttime and show no significant diurnal variations. While in Delta, the TGM concentrations are higher in daytime but lower in nighttime. These observed diurnal patterns are all well reproduced by the model. Fig. S13 shows the simulated averaged diurnal variation of surface TGM concentrations in Mt. Lulin (2862 m a.s.l.), Mt. Leigong (2178 m a.s.l.) and Mt. Changbai (741 m a.s.l.) in China. In Mt. Lulin, the simulated TGM concentrations exhibit a clear diurnal pattern, with higher concentrations in daytime but lower concentrations in nighttime. The daily maxima occurs in the afternoon. This simulated pattern is consistent with the observed results reported by Sheu et al. (2010). And they pointed out that this diurnal variation resulted from upslope movement of boundary layer air in daytime and subsidence of free troposphere air at night. The variation of TGM concentrations in Mt. Leigong is similar to that in Mt. Lulin and also agree with filed observations (Fu et al., 2010c). In Mt. Changbai, the diurnal variation of TGM shows different pattern. TGM peaks after sunrise and then decrease to the valley in

the afternoon. Fu et al. (2012b) concluded that this variation was caused by regional transport.

Fig. S14 shows the vertical distribution of TGM concentrations derived from aircraft observations and model simulation over East Asia. The aircraft observations show two maxima, one near ground and the other at 6-7 km. The model reproduces the strong near ground TGM enhancement driven by continental outflow. However, the simulated TGM shows a monotonic decrease with altitude, and does not reproduce the observed 6-7 km enhancement. Friedli et al. (2004) pointed out that this high-altitude TGM enhancement was associated with lofted pollution from unknown sources or returning Asian plums after having circled the globe. Fig. S15 illustrates the simulated averaged vertical variation of TGM concentrations over the North Pacific Ocean (NPO) during April-May 2001. TGM concentrations over the south and north parts of NPO show similar vertical patterns. The highest concentrations are found at surface and then slowly decrease with altitude. At all levels, higher TGM concentrations occur over the north part of NPO which is related to long-range transport of Hg(0) from mainland in middle latitude. These simulated results agree with aircraft observations conducted in the INTEX-B filed experiment (Singh et al., 2009) and are also comparable to the simulated results from GEOS-Chem (Holmes et al., 2010).

The above comparisons confirm the model capability of simulating the diurnal and vertical variations of TGM.

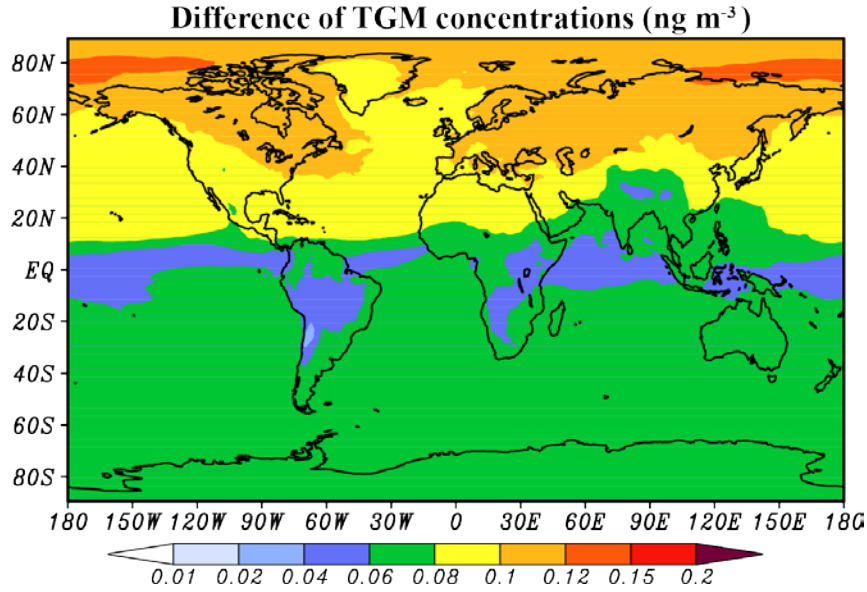

Fig. S1. Change in surface TGM concentrations (ng m^{-3}) by introducing bromine chemistry (positive value means the TGM concentrations decrease after added bromine chemistry).

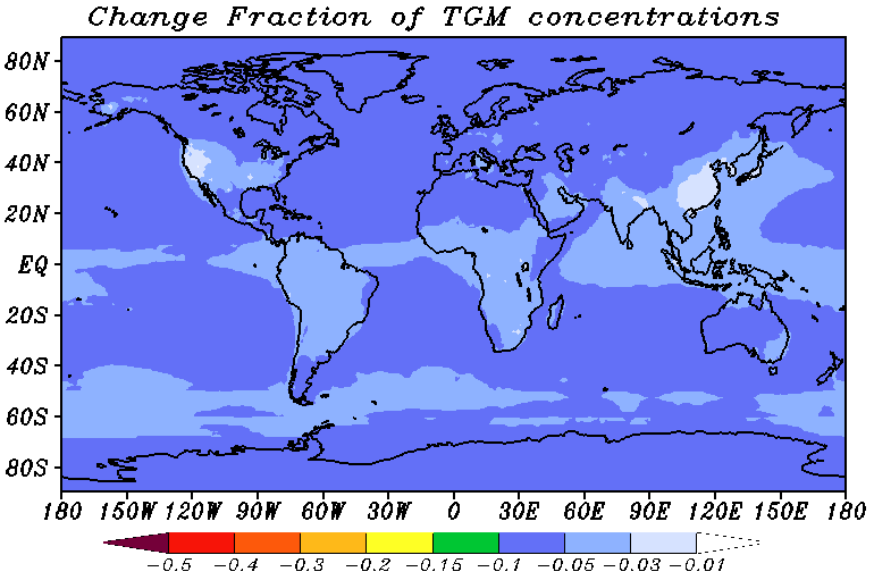

Fig. S2. Change fraction (unitless) of surface TGM concentrations by introducing the mechanism of gas-particle partitioning of Hg(II) (negative value means the TGM concentrations decrease after introducing the mechanism).

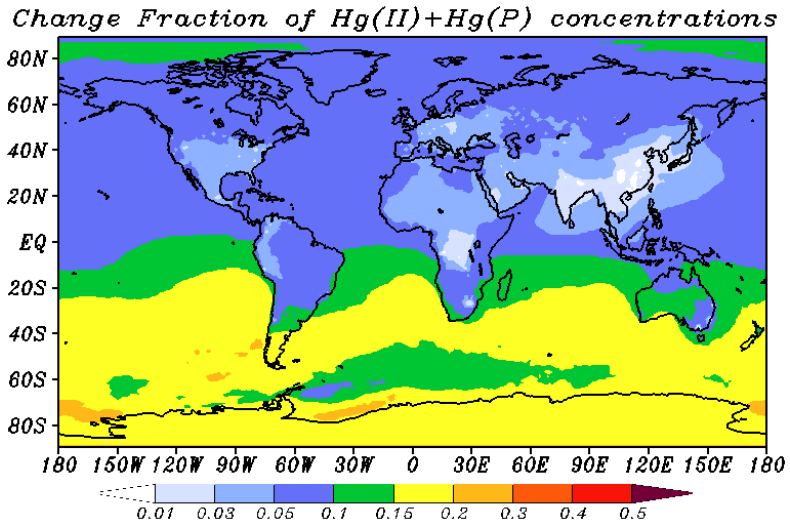

Fig. S3. Change fraction (unitless) of surface Hg(II)+Hg(P) concentrations by introducing the mechanism of gas-particle partitioning of Hg(II) (positive value means the Hg(II)+Hg(P) concentrations increase after introducing the mechanism).

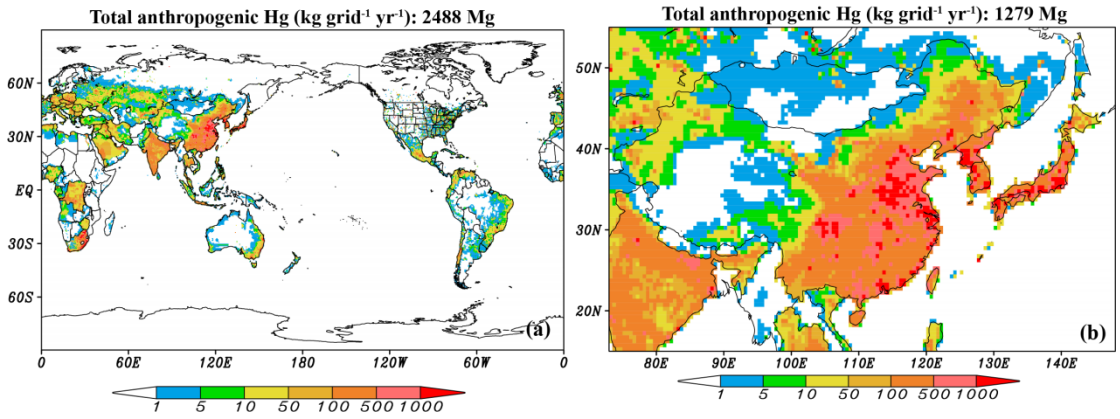

Fig. S4. Global (a) and East Asia (b) annual anthropogenic Hg emissions (kg grid^{-1} yr^{-1}).

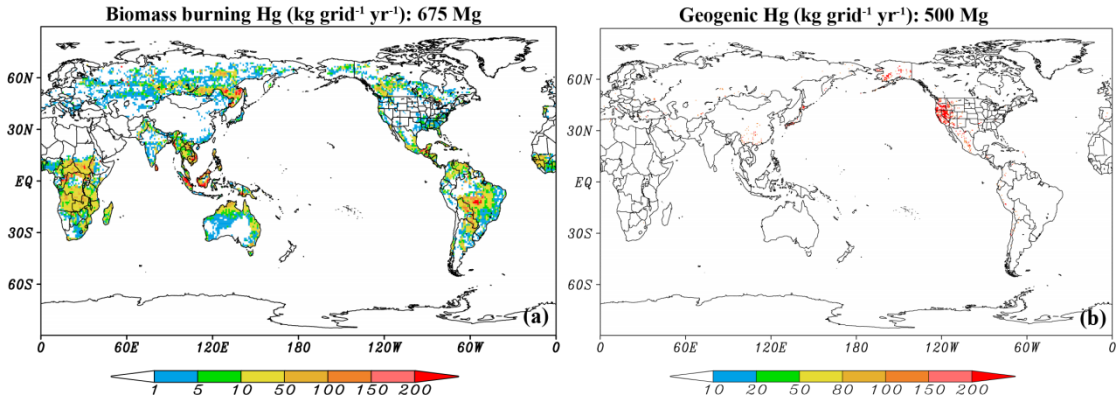

Fig. S5. Global annual biomass burning (a) and geogenic (b) Hg emissions (kg grid^{-1} yr^{-1}).

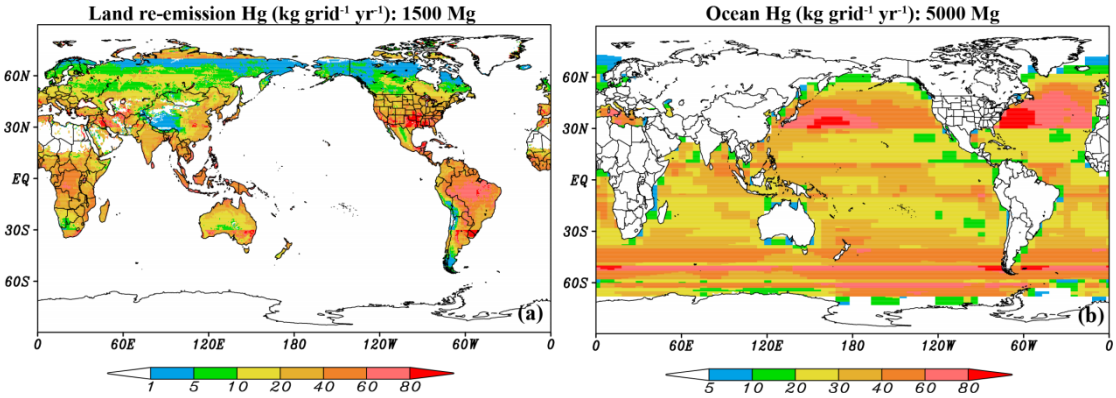

Fig. S6. Global annual land re-emission (a) and total ocean emissions (b) of Hg (kg grid^{-1} yr^{-1}).

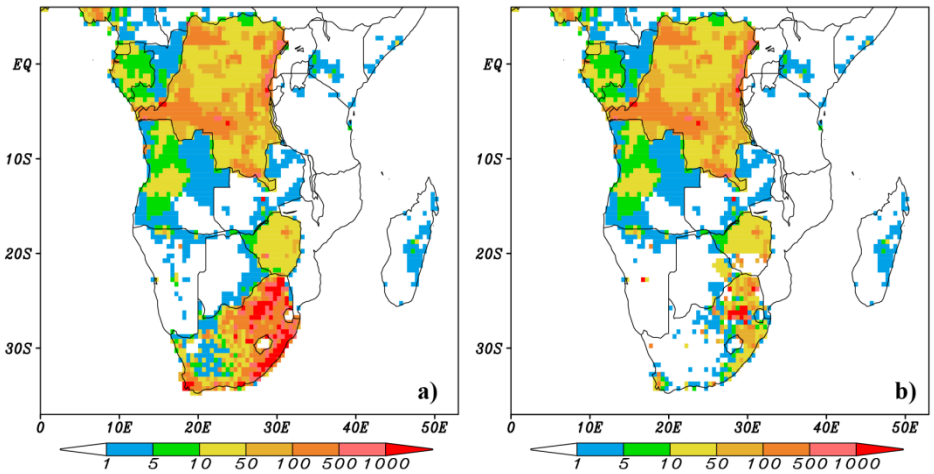

Figure S7. Annual anthropogenic Hg emissions (kg grid^{-1} yr^{-1}) in South Africa, a) the AMAP 2000 inventory and b) the AMAP 2010 inventory in South Africa (16-34^{0}E, 36-20^{0}S) + the AMAP 2000 inventory elsewhere.

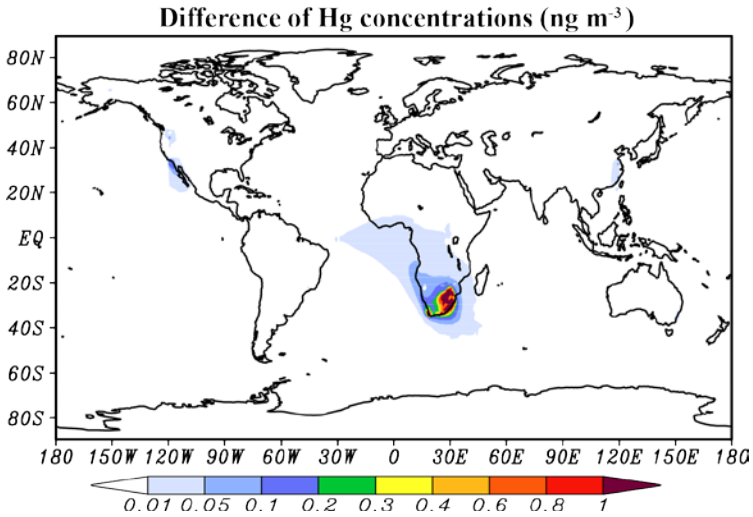

Figure S8. Difference of global surface Hg concentrations (ng m^{-3}) after updating the anthropogenic emissions in South Africa by using the AMAP 2010 inventory.

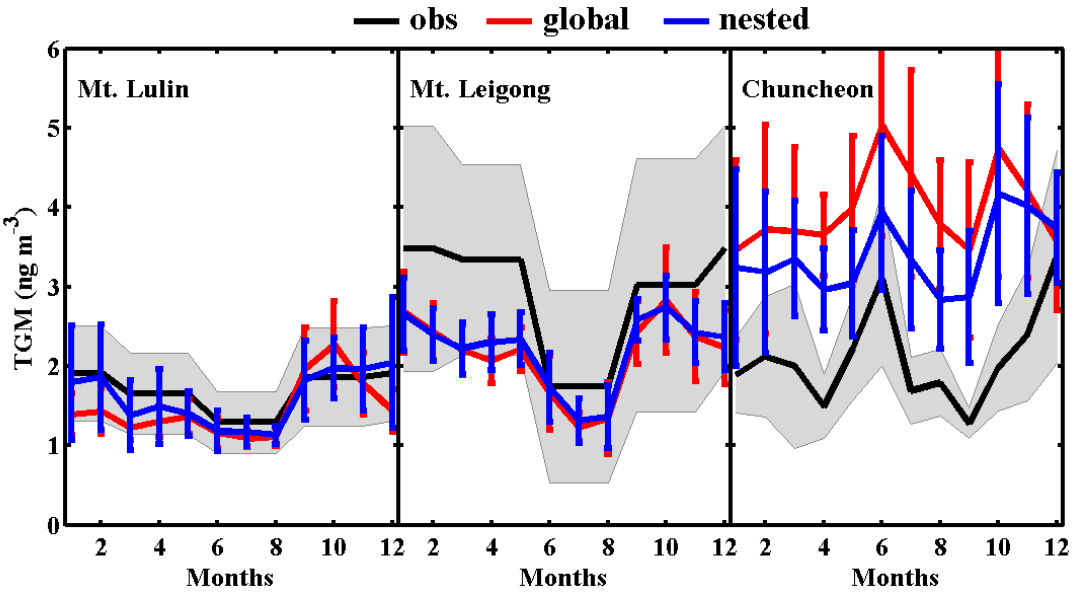

Fig. S9. Mean seasonal variation of TGM (ng m^{-3}) in Mt. Lulin and Mt. Leigong in China, and Chuncheon in Korea. Shaded areas and vertical bars show one standard deviation for observations and for model results.

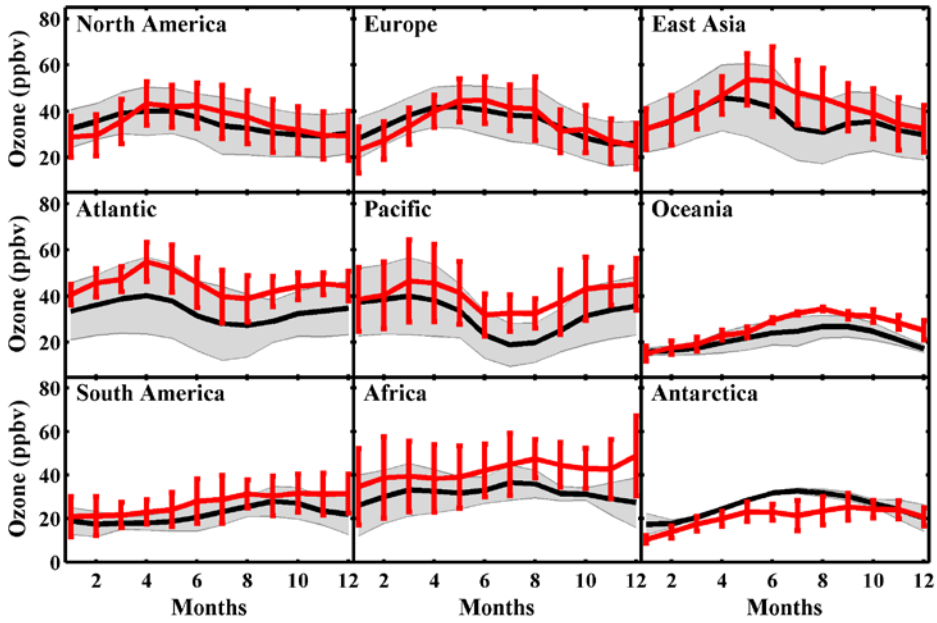

Fig. S10. Mean seasonal variation of surface ozone (ppbv) at 9 subregions in 2001. Gray shaded areas and red vertical bars show one standard deviation over the sites for observations and for model results. Observations are from the WDCGG (World Data Centre for Greenhouse Gases) and EANET (Acid Deposition Monitoring Network in East Asia) network.

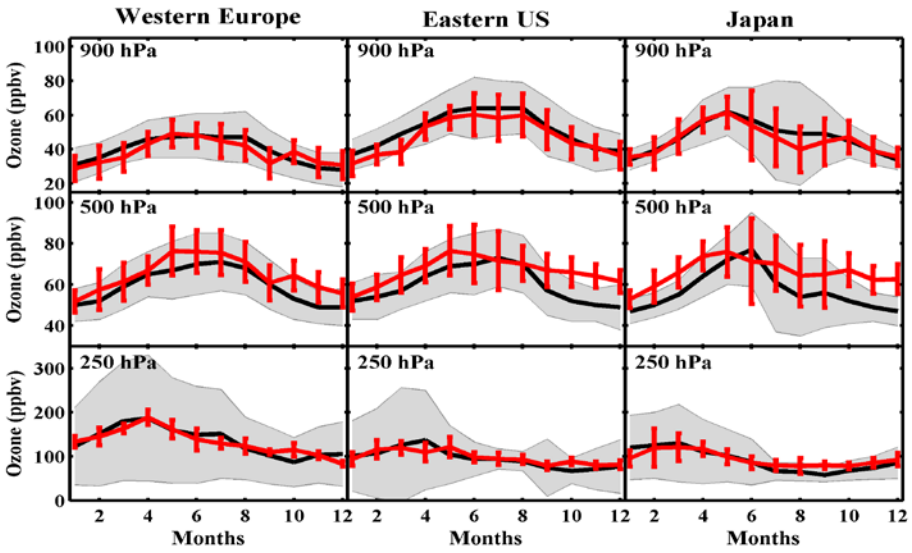

Fig. S11. Comparison of the ozone (ppbv) seasonal cycle between ozonesonde observations (black lines) and model results (red lines) in 900, 500 and 250 hPa in Western Europe, Eastern US and Japan. Gray shaded areas and red vertical bars show one standard deviation over the ozonesonde locations for observations and for model results. Observations are from Tilmes et al. (2012).

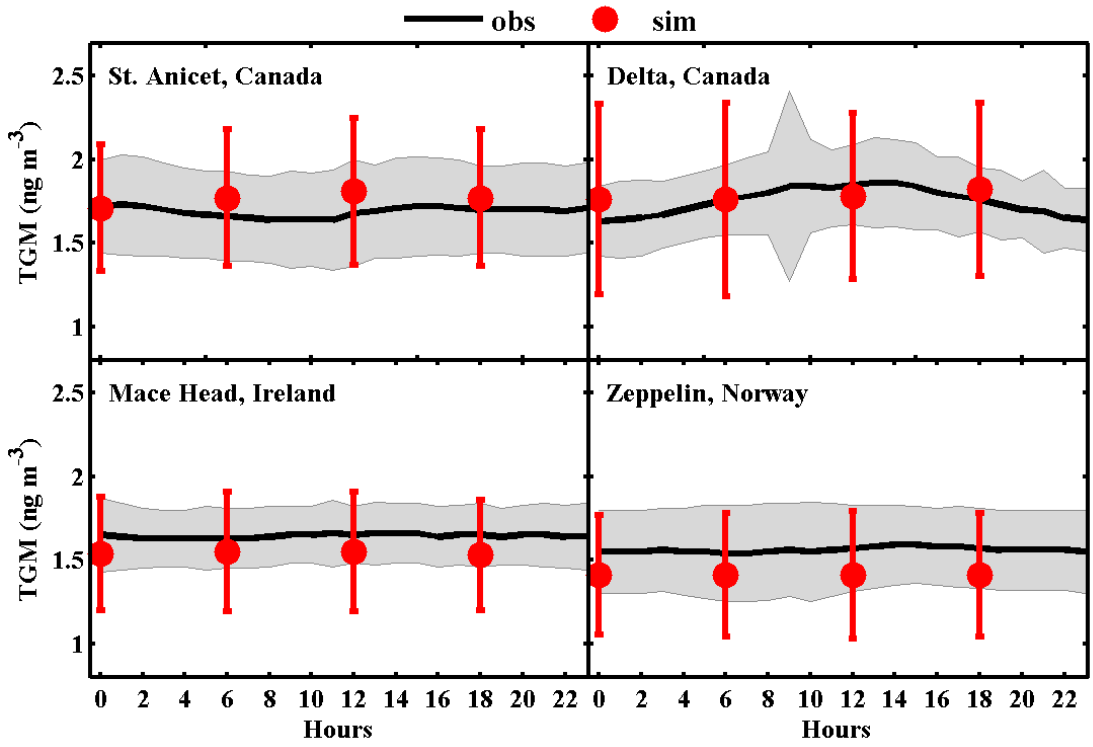

Fig. S12. Mean diurnal variation of TGM (ng m^{-3}) in St. Anicet, Delta, Mace Head, and Zeppelin in 2001. Gray shaded areas and red vertical bars show one standard deviation for observations and for model results. Note that the output frequency of the global simulation is 6 hours.

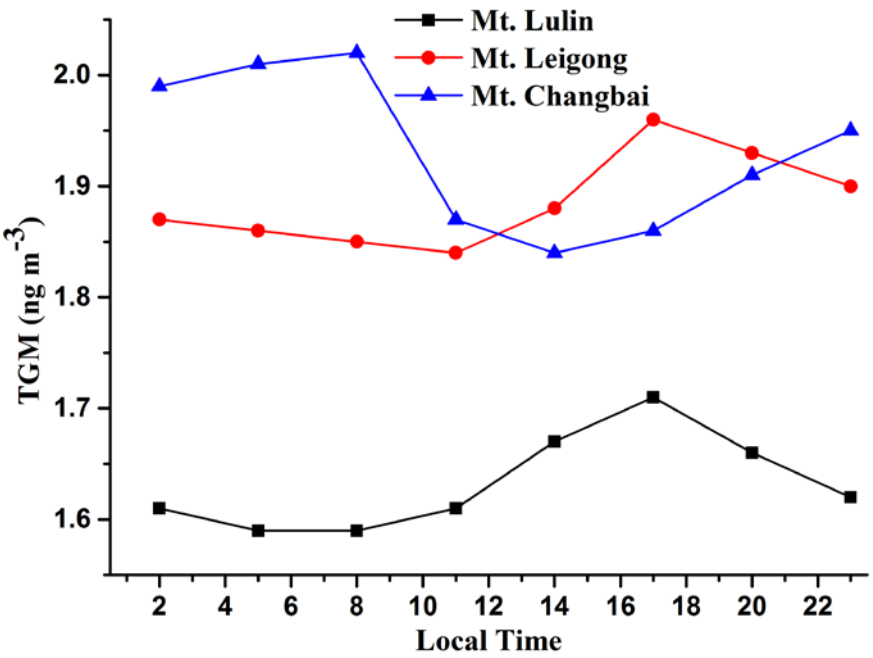

Fig. S13. Simulated averaged diurnal variation of surface TGM concentrations (ng m^{-3}) in Mt. Lulin, Mt. Leigong and Mt. Changbai in 2001.

.

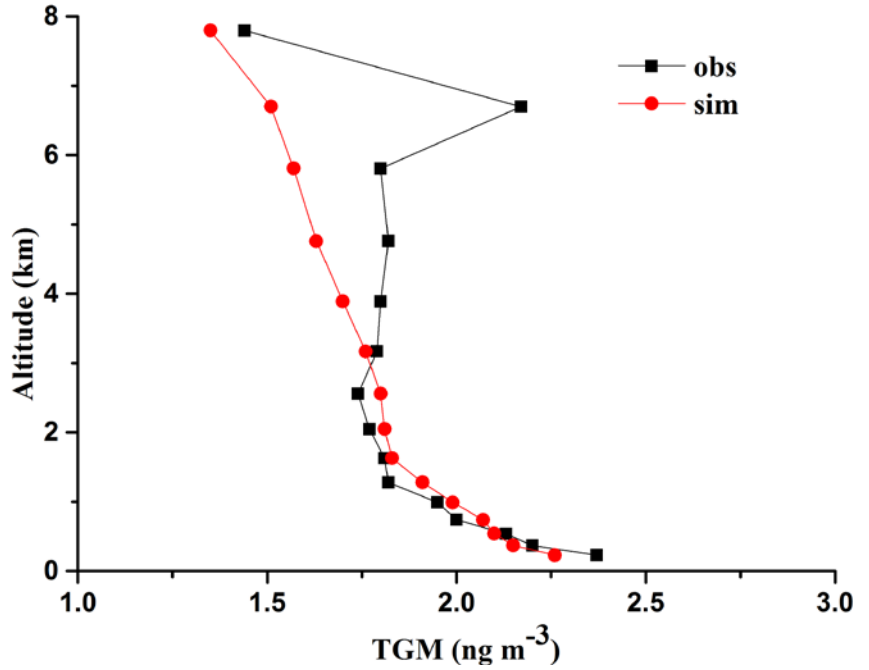

Fig. S14. Vertical variation of TGM concentrations (ng m^{-3}) over East Asia (24-42°N, 124-144°E) in April 2001. Observations are from the ACE-Asia aircraft campaign in April 2001 (Friedli et al., 2004). The observations are averaged according to each model layer height and depth.

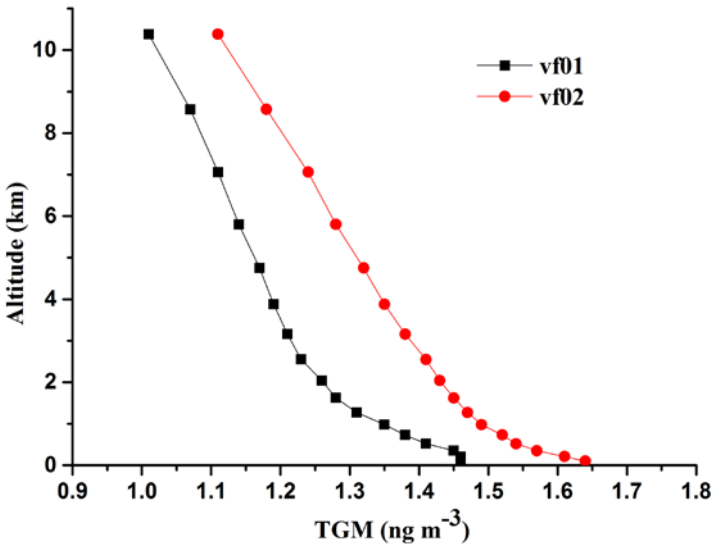

Fig. S15. Simulated averaged vertical variation of TGM concentrations (ng m^{-3}) over the North Pacific Ocean during April-May 2001. vf01 and vf02 stand for the vertical profile of TGM averaged over (19-25 °N, 120° E-120° W) and (30-55°N, 150°E-150°W) respectively.

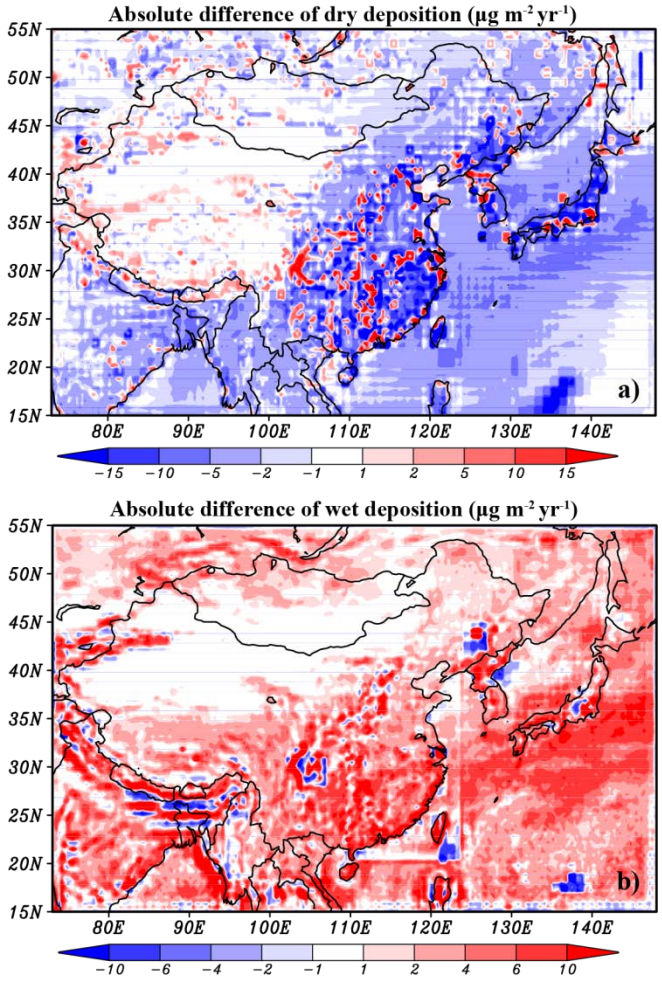

Figure S16. Absolute differences of annual dry and wet deposition (μg m^{-2} yr^{-1}) over East Asia between the global and nested simulations (Nested-Global).

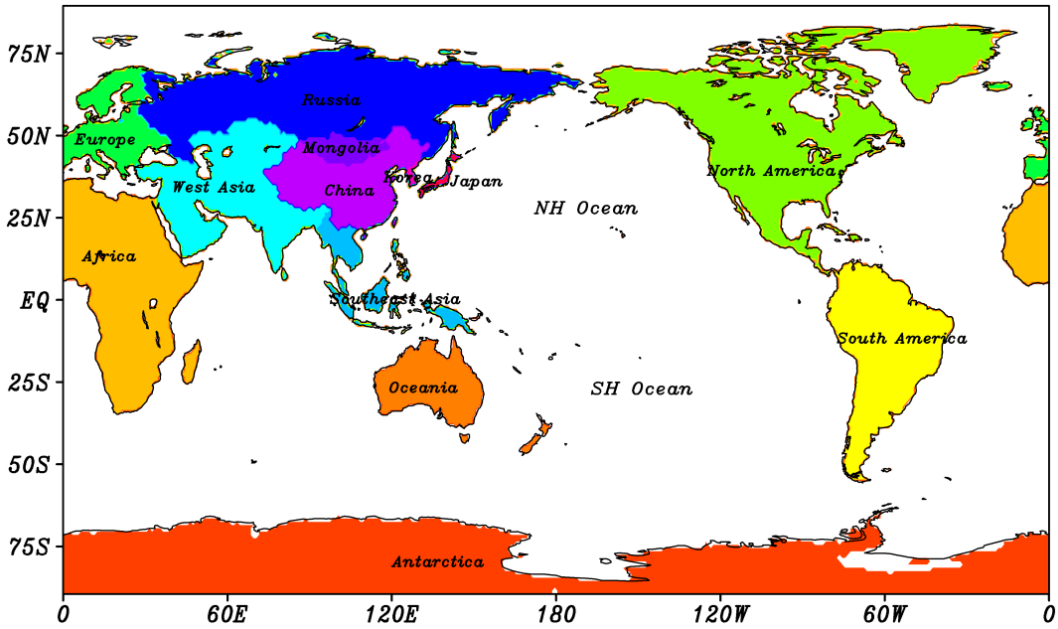

Fig. S17. 15 geographical areas used in this study, colors represent subregions over land while ocean is divided into two parts used the equator as boundary.

Table S1. Bromine reactions added in the model (T is the temperature in degrees Kelvin, and P is the pressure in atmospheres).

NO.	Reaction	Rates
BR1	Hg(0)(g)+Br(g)→HgBr(g)	$k1 = 3.6 \times 10^{-13} P \left(\frac{T}{298}\right)^{-1.86}$ $cm^3\,molec^{-1}\,s^{-1}$
BR2	HgBr(g)→Hg(0)(g)	$k2 = 3.9 \times 10^{9} exp\left(\frac{-8537}{T}\right)$ s^{-1}
BR3	HgBr(g)+Br(g)→$HgBr_2$(g)	$k3 = 2.5 \times 10^{-10} \left(\frac{T}{298}\right)^{-0.57}$ $cm^3\,molec^{-1}\,s^{-1}$
BR4	HgBr(g)+OH(g)→HgBrOH(g)	$k4 = 2.5 \times 10^{-10} \left(\frac{T}{298}\right)^{-0.57}$ $cm^3\,molec^{-1}\,s^{-1}$
BR5	Hg(0)(g)+BrO(g)→Hg(II)(g)	$k5 = 1.0 \times 10^{-15}$ $cm^3\,molec^{-1}\,s^{-1}$

Table S2. Long-term TGM/GEM measurements used for model evaluation (ng m^{-3}).

Site[a]	Years	Conc[b]	Reference
Alert, Canada (83N, 62W)*	1995-2002	1.55	Environment Canada (2003)
FortChipewyan, Canada (59N, 111W)	2000-2001	1.36	Temme et al. (2007)
Kuujjuarapik, Canada (56N, 78W) *	1999-2000	1.82#	Steffen et al. (2005)
Esther, Canada (52N, 110W)	1997-1999	1.65	Kellerhals et al. (2003)
Mingan, Canada (50N, 64W)	1997-1999	1.62	Kellerhals et al. (2003)
Bratts Lake, Canada (50N, 105W)	2001-2005	1.53	Temme et al. (2007)
Reifel Island, Canada (49N, 123W)*	1997-1999	1.67	Kellerhals et al. (2003)
Delta, Canada (49N, 123W)	1999-2001	1.73	Environment Canada (2003)
Burnt Island, Canada (46N, 83W)	1997-1999	1.58	Kellerhals et al. (2003)
St.Andrews, Canada (45N, 67W)*	1997-1999,2001	1.42	Environment Canada (2003)
St.Anicet, Canada (45N, 74W)*	1997-1999,2001	1.64	Kellerhals et al. (2003); Poissant et al. (2005)
Kejimkujik, Canada (44N, 65W)*	2001	1.45	Environment Canada (2003)
Egbert, Canada (44N, 80W)	1997-1999	1.67	Kellerhals et al. (2003)
Pt.Petre, Canada (44N, 77W)	1997-1999	1.78	Kellerhals et al. (2003)
Cheeka Peak, USA (48N, 125W) *	2001-2002	1.56	Weiss-Penzias et al. (2003)
NewcombNY, USA (43N, 74W) *	2006-2007	1.45	Choi et al. (2008)
PacMonadnock, USA (43N, 72W) *	2007	1.38#	Sigler et al. (2009)
RenoDRI, USA (40N, 120W)*	2002-2005	2.10	Stamenkovic et al. (2007)
AthensOH, USA (39N, 82W) *	2004-2005	1.63#	Yatavelli et al. (2006)
PensacolaOLF, USA (31N, 87W) *	2004-2006	1.34#	Edgerton et al. (2006)
Pallas, Finland (68N, 24E)*	1998-2002	1.38	EMEP (2005)
Zingst, Germany (55N, 13E)*	2000	1.64	EMEP (2005)
Neuglobsow, Germany (53N, 13E)*	2004-2005	1.70	EMEP (2009)
Langenbruegge, Germany (53N, 11E)*	2002	1.98	EMEP (2005)
Mace Head, Ireland (54N, 10W)*	1995-2001	1.69	Ebinghaus et al. (2002)
SanLucido, Italy (39N, 16E)	2004-2005	1.80	EMEP (2009)
Zeppelin, Norway (79N, 12E)*	2000-2004	1.58	EMEP (2005)
Andoya, Norway (69N, 16E)*	2004	1.66	EMEP (2009)
Birkenes, Norway (58N, 8E)*	2005-2007	1.82	EMEP (2009)
Lista, Norway (58N, 7E)*	2000-2003	1.70	EMEP (2005)
Amderma, Russia (70N, 62E) *	2001-2003	1.66#	Steffen et al. (2005)
CaboDeCreus, Spain (42N, 3E)*	2005	1.73	EMEP (2009)
Rao, Sweden (57N, 12E)*	2001	1.66	EMEP (2005)
Rorvik, Sweden (57N, 12E)*	2001-2002	1.66	EMEP (2005)
Cape Point, South Africa (34S, 19E)*	1998-2002, 2007-2008	1.22	Baker et al. (2002); Slemr et al. (2011)
Neumayer, Antarctica (70S, 8W)*	2000	1.06	Ebinghaus et al. (2002)
Changchun, China (44N, 125E)	1999-2000	15.10	Fang et al. (2004)
ChangbaiMt, China (42N, 129E)	2005-2006	3.15	Wan et al. (2009a)
Beijing, China (40N, 116E)	2005	6.60#	Wang et al. (2007)
Chengshantou, China (37N, 123E)	2007-2009	2.17#	Ci et al. (2011a)

Table S2. Continued.

Site[a]	Years	Conc[b]	Reference
Waliguan,China (36N, 101E)	2007-2008	1.98	Fu et al. (2012a)
Shanghai, China (31N, 121E)	2008-2010	7.79	Zhang et al. (2012)
GonggaMt, China (30N, 102E)	2005-2006	3.89	Fu et al. (2008a)
Chongqing, China (30N, 107E)	2006-2007	6.74#	Yang et al. (2009)
Shangri-La, China (28N, 100E)	2009-2010	2.59	Zhang (2011)
Guiyang, China (27N, 107E)	2001-2002	6.95	Feng et al. (2004)
LeigongMt, China (26N, 108E) *	2008-2009	3.03#	Fu et al. (2010c)
LulinMt, China (24N, 121E) *	2006-2007	1.62#	Sheu et al. (2010)
Guangzhou, China (23N, 113E)	2010-2011	4.86	Liu et al. (2012)
Tokyo, Japan (36N, 140E)	2000-2001	2.70	Sakata and Marumoto (2002);
Chiba, Japan (36N, 140E)	1991-1996	11.90	Nakagawa and Hiromoto (1997)
Hayama, Japan (35N, 140E)	1991-1996	13.20	Nakagawa and Hiromoto (1997)
Chuncheon, Korea (38N, 127E)*	2006-2009	2.11	Holmes et al. (2010)
Seoul, Korea (37N, 127E)	1997-2002	4.42	Kim et al. (2005)
Kanghwa, Korea (37N, 126E)	2008-2009	1.92	Han et al. (2011)
An-Myun,Korea (37N, 126E)	2005	4.27	Nguyen et al. (2007)
Jeju Island, Korea (33N, 126E)	2006-2007	3.58	Nguyen et al. (2010)

[a] Asterisk indicates that monthly mean observations are also available from the references.

[b] Pound sign indicates GEM measurements.

Table S3. Mercury measurements from ship cruises used for model evaluation.

Cruise	Region	Date	Obs	Reference
Lamborg1999	South and equatorial Atlantic Ocean	May to Jun, 1996	TGM	Lamborg et al. (1999)
Temme2003	Atlantic Ocean	Feb 2001	TGM	Temme et al. (2003)
Laurier2003	North Pacific Ocean	May to Jun, 2002	TGM/RGM	Laurier et al. (2003)
Soerensen2010	Notrh Atlantic, Indian Ocean, South Pacific	Aug 2006 to Apr 2007	GEM	Soerensen et al. (2010)
Fu2010	South China Sea	Aug 2008	GEM	Fu et al. (2010a)
Ci2011	Yellow Sea	Jul 2010	GEM	Ci et al. (2011b)

Table S4. Long-term RGM and TPM measurements used for model evaluation (pg m^{-3})[a].

Site	RGM	TPM	Total	Period	Reference
St.Anicet, Canada (45N, 74W)	3	26	29	2003	Poissant et al. (2005)
Barrow, USA (71N, 157W)	24	NA	24	1999-2001	Landis et al. (2002)
Potsdam, USA (45N, 75W)	4.2	NA	4.2	2002-2003	Han et al. (2005)
Sterling, USA (43N, 77W)	6	NA	6	2002-2003	Han et al. (2005)
Stockton, USA (42N, 79W)	5.7	NA	5.7	2002-2003	Han et al. (2005)
Durham, USA (36N, 79W)	16	NA	16	1999-2001	Landis et al. (2002)
Baltimore, USA (32N, 77W)	23	NA	23	1999-2001	Landis et al. (2002)
Everglades, USA (26N, 81W)	15	NA	15	1999-2001	Landis et al. (2002)
Zingst, Germany (55N, 13E)	25	22	47	1998-1999	Munthe et al. (2003)
Neuglobsow, Germany (53N, 13E)	18	25	43	1998-1999	Munthe et al. (2003)
Mace Head, Ireland (54N, 10W)	18	5	23	1998-1999	Munthe et al. (2003)
Avspreten, Sweden (58N, 17E)	8	9	17	1998-1999	Munthe et al. (2003)
Rorvik, Sweden (57N, 12E)	15	5	20	1998-1999	Munthe et al. (2003)
Changchun, China (44N, 125E)	NA	192.5	192.5	1999-2000	Fang et al. (2004)
ChangbaiMt, China (42N, 129E)	65	77	142	2005-2006	Wan et al. (2009b)
Beijing, China (40N, 116E)	NA	930	930	2003-2004	Wang et al. (2006)
Waliguan,China (36N, 101E)	7.4	19.4	26.8	2007-2008	Fu et al. (2012a)
Hefei, China (32N, 117E)	NA	330	330	2008-2009	Wang (2010)
Shanghai, China (31N, 121E)	NA	560	560	2004-2006	Xiu et al. (2009)
GonggaMt, China (30N, 102E)	6.2	30.7	36.9	2005-2006	Fu et al. (2008b)
Chongqing, China (30N, 107E)	NA	416	416	2005	Wu (2006)
Shangri-La, China (28N, 100E)	8.2	43.5	51.7	2009-2010	Zhang (2011)
Guiyang, China (27N, 107E)	35.7	368	403.7	2009	Fu et al. (2011)
LulinMt, China (24N, 121E)	12.1	2.3	14.4	2006-2007	Sheu et al. (2010)
Seoul, Korea (38N, 127E)	27.2	23.9	51.1	2005-2006	Kim et al. (2009)
Tokyo, Japan (36N, 140E)	NA	98	98	2000-2001	Sakata and Marumoto (2002)

[a] The sum of RGM and TPM is defined as total oxidized mercury and compared to the sum of Hg(II)+Hg(P) in the model.

Table S5. Long-term dry and wet depositions measurements in East Asia used for model evaluation (Units for deposition and precipitation are μg m^{-2} yr^{-1} and mm yr^{-1}).

Site	Lat	Lon	Period	Dry	Wet	Prec	Reference
ChangbaiMt, China	42.4	128.5	2005-2006	16.5	8.4	613	Wan et al. (2009b)
Changchun, China	43.8	125.4	1999-2000	131.8	108.0	567	Fang et al. (2004)
Beijing, China	40.1	116.3	2003	338.3	NA	NA	Wang et al. (2006)
Shanghai, China	31.4	121.4	2008-2009	NA	250.5	947	Zhang et al. (2010)
Chongqin, China	29.6	104.7	2005-2006	256.0	77.6	1403	Wang et al. (2009)
GonggaMt, China	29.6	102.2	2005-2007	66.4	26.1	1818	Fu et al. (2010b)
Wujiang, China	26.5	106.1	2006	NA	34.7	963	Guo et al. (2008)
LeigongMt, China	26.4	108.2	2005-2006, 2008-2009	44.0	16.2	1437	Fu et al. (2010c) Wang et al. (2009)
Bekkai, Japan	43.4	145.1	2002-2003	4.4	5.8	1117	Sakata and Marumoto (2005)
Hayakita, Japan	42.7	141.6	2002-2003	5.2	7.1	882	Sakata and Marumoto (2005)
Akita, Japan	40.2	140.0	2002-2003	9.4	14.9	1576	Sakata and Marumoto (2005)
Fukushima, Japan	37.6	140.7	2002-2003	6.8	10.0	1599	Sakata and Marumoto (2005)
Ishikawa, Japan	37.2	136.9	2002-2003	6.6	14.2	2076	Sakata and Marumoto (2005)
Tokyo, Japan	35.6	139.6	2002-2003	NA	16.7	1912	Sakata and Marumoto (2005)
Aichi, Japan	35.0	137.5	2002-2003	13.2	13.1	1679	Sakata and Marumoto (2005)
Hyogo, Japan	34.8	134.8	2002-2003	8.2	14.0	1481	Sakata and Marumoto (2005)
Hiroshima, Japan	34.4	132.7	2002-2003	9.7	14.3	1624	Sakata and Marumoto (2005)
Nagasaki, Japan	33.3	129.7	2002-2003	8.3	17.7	2317	Sakata and Marumoto (2005)
Korea	35.9	127.8	2006-2008	NA	9.4	1068	Ahn et al. (2011)

Table S6. Hg budgets over East Asia (15-55°N, 75-145°E) in the global and nested simulations (Unit: Mg yr^{-1}).

	global domain	nested domain	nested/global
Total Sources	1461	1461	1.00
anthropogenic	979	979	1.00
land	269	269	1.00
ocean	213	213	1.00
Total Sinks	824	843	1.02
Wet deposition	182	278	1.53
Dry deposition	642	565	0.88
TGM burden	548	512	0.93

References

Ahn, M. C., Yi, S. M., Holsen, T. M., and Han, Y. J.: Mercury wet deposition in rural Korea: concentrations and fluxes, J. Environ. Monit., 13, 2748-2754, doi:10.1039/c1em10014a, 2011.

AMAP/UNEP: Technical Background Report to the Global Atmospheric Mercury Assessment, Tech. rep., Arctic Monitoring and Assessment Programme / UNEP Chemicals Branch, http: //www.unep.org/hazardoussubstances/, 2008.

Baker, P. G. L., Brunke, E. G., Slemr, F., and Crouch, A. M.: Atmospheric mercury measurements at Cape Point, South Africa, Atmos. Environ., 36, 2459-2465, 2002.

Bullock, O. R., and Brehme, K. A.: Atmospheric mercury simulation using the CMAQ model: formulation description and analysis of wet deposition results, Atmos. Environ., 36, 2135-2146, doi:10.1016/s1352-2310(02)00220-0, 2002.

CAMx: CAMx, user's guide, version 6.1, Environ International Corporation, California, 2014.

Choi, H. D., Holsen, T. M., and Hopke, P. K.: Atmospheric mercury (Hg) in the Adirondacks: Concentrations and sources, Environ. Sci. Technol., 42, 5644-5653, doi:10.1021/es7028137, 2008.

Ci, Z., Zhang, X., Wang, Z., and Niu, Z.: Atmospheric gaseous elemental mercury (GEM) over a coastal/rural site downwind of East China: Temporal variation and long-range transport, Atmos. Environ., 45, 2480-2487, doi:10.1016/j.atmosenv.2011.02.043, 2011a.

Ci, Z., Zhang, X., Wang, Z., Niu, Z., Diao, X., and Wang, S.: Distribution and air-sea exchange of mercury (Hg) in the Yellow Sea, Atmos. Chem. Phys., 11, 2881-2892, doi:10.5194/acp-11-2881-2011, 2011b.

Clever, H. L., Johnson, S. A., and Derrick, M. E.: The solubility of mercury and some sparingly soluble mercury salts in water and aqueous-electrolyte solutions, J. Phys. Chem. Ref. Data, 14, 631-681, 1985.

Ebinghaus, R., Kock, H. H., Temme, C., Einax, J. W., Lowe, A. G., Richter, A., Burrows, J. P., and Schroeder, W. H.: Antarctic springtime depletion of atmospheric mercury, Environ. Sci. Technol., 36, 1238-1244, doi:10.1021/es015710z, 2002.

Edgerton, E. S., Hartsell, B. E., and Jansen, J. J.: Mercury speciation in coal-fired power plant plumes observed at three surface sites in the southeastern US, Environ. Sci. Technol., 40, 4563-4570, doi:10.1021/es0515607, 2006.

Fang, F., Wang, Q., and Li, J.: Urban environmental mercury in Changchun, a metropolitan city in Northeastern China: source, cycle, and fate, Sci. Total Environ., 330, 159-170, doi:10.1016/j.scitotenv.2004.04.006, 2004.

Feng, X., Shang, L., Wang, S., Tang, S., and Zheng, W.: Temporal variation of total gaseous mercury in the air of Guiyang, China, J. Geophys. Res.-Atmos., 109, D03303, doi:10.1029/2003jd004159, 2004.

Fu, X., Feng, X., Zhu, W., Wang, S., and Lu, J.: Total gaseous mercury concentrations in ambient air in the eastern slope of Mt. Gongga, South-Eastern fringe of the Tibetan plateau, China, Atmos. Environ., 42, 970-979, doi:10.1016/j.atmosenv.2007.10.018, 2008a.

Fu, X., Feng, X., Zhu, W., Zheng, W., Wang, S., and Lu, J. Y.: Total particulate and reactive gaseous mercury in ambient air on the eastern slope of the Mt. Gongga area, China, Appl. Geochem., 23, 408-418, doi:10.1016/j.apgeochem.2007.12.018, 2008b.

Fu, X., Feng, X., Zhang, G., Xu, W., Li, X., Yao, H., Liang, P., Li, J., Sommar, J., Yin, R., and Liu,

N.: Mercury in the marine boundary layer and seawater of the South China Sea: Concentrations, sea/air flux, and implication for land outflow, J. Geophys. Res.-Atmos., 115, D06303, doi:10.1029/2009jd012958, 2010a.

Fu, X., Feng, X., Zhu, W., Rothenberg, S., Yao, H., and Zhang, H.: Elevated atmospheric deposition and dynamics of mercury in a remote upland forest of southwestern China, Environ. Pollut., 158, 2324-2333, doi:10.1016/j.envpol.2010.01.032, 2010b.

Fu, X., Feng, X., Qiu, G., Shang, L., and Zhang, H.: Speciated atmospheric mercury and its potential source in Guiyang, China, Atmos. Environ., 45, 4205-4212, doi:10.1016/j.atmosenv.2011.05.012, 2011.

Fu, X., Feng, X., Dong, Z., Yin, R., Wang, J., Yang, Z., and Zhang, H.: Atmospheric gaseous elemental mercury (GEM) concentrations and mercury depositions at a high-altitude mountain peak in south China, Atmos. Chem. Phys., 10, 2425-2437, 2010c.

Fu, X., Feng, X., Liang, P., Deliger, Zhang, H., Ji, J., and Liu, P.: Temporal trend and sources of speciated atmospheric mercury at Waliguan GAW station, Northwestern China, Atmos. Chem. Phys., 12, 1951-1964, doi:10.5194/acp-12-1951-2012, 2012a.

Fu, X. W., Feng, X., Shang, L. H., Wang, S. F., and Zhang, H.: Two years of measurements of atmospheric total gaseous mercury (TGM) at a remote site in Mt. Changbai area, Northeastern China, Atmos. Chem. Phys., 12, 4215-4226, doi:10.5194/acp-12-4215-2012, 2012b.

Friedli, H. R., Radke, L. F., Prescott, R., Li, P., Woo, J. H., and Carmichael, G. R.: Mercury in the atmosphere around Japan, Korea, and China as observed during the 2001 ACE-Asia field campaign: Measurements, distributions, sources, and implications, J. Geophys. Res.-Atmos., 109, D19s25, doi:10.1029/2003jd004244, 2004.

Guo, Y., Feng, X., Li, Z., He, T., Yan, H., Meng, B., Zhang, J., and Qiu, G.: Distribution and wet deposition fluxes of total and methyl mercury in Wujiang River Basin, Guizhou, China, Atmos. Environ., 42, 7096-7103, doi:10.1016/j.atmosenv.2008.06.006, 2008.

Han, J. S., Choi, E. M., Seo, Y. S., Yi, S. M., Lee, J., and Chung, Y. C.: Contribution of total gaseous mercury (TGM) using TGM concentrations measured in urban and background areas, Korea, 10th International Conference on Mercury as a Global Pollutant, Halifax, Nova Scotia, Canada, 2011.

Han, Y. J., Holsen, T. M., Hopke, P. K., and Yi, S. M.: Comparison between back-trajectory based modeling and Lagrangian backward dispersion Modeling for locating sources of reactive gaseous mercury, Environ. Sci. Technol., 39, 1715-1723, doi:10.1021/es0498540, 2005.

Holmes, C. D., D. J. Jacob and X. Yang: Global lifetime of elemental mercury against oxidation by atomic bromine in the free troposphere. Geophysical Research Letters 33(20): L20808, 2006.

Holmes, C. D., Jacob, D. J., Corbitt, E. S., Mao, J., Yang, X., Talbot, R., and Slemr, F.: Global atmospheric model for mercury including oxidation by bromine atoms, Atmos. Chem. Phys., 10, 12037-12057, doi:10.5194/acp-10-12037-2010, 2010.

Kellerhals, M., Beauchamp, S., Belzer, W., Blanchard, P., Froude, F., Harvey, B., McDonald, K., Pilote, M., Poissant, L., Puckett, K., Schroeder, B., Steffen, A., and Tordon, R.: Temporal and spatial variability of total gaseous mercury in Canada: results from the Canadian Atmospheric Mercury Measurement Network (CAMNet), Atmos. Environ., 37, 1003-1011, doi:10.1016/s1352-2310(02)00917-2, 2003.

Kim, K. H., Ebinghaus, R., Schroeder, W. H., Blanchard, P., Kock, H. H., Steffen, A., Froude, F.

A., Kim, M. Y., Hong, S. M., and Kim, J. H.: Atmospheric mercury concentrations from several observatory sites in the northern hemisphere, J. Atmos. Chem., 50, 1-24, doi:10.1007/s10874-005-9222-0, 2005.

Kim, S. H., Han, Y. J., Holsen, T. M., and Yi, S. M.: Kim, S. H., Han, Y. J., Holsen, T. M., and Yi, S. M.: Characteristics of atmospheric speciated mercury concentrations (TGM, Hg(II) and Hg(p)) in Seoul, Korea, Atmos. Environ., 43, 3267-3274, doi:10.1016/j.atmosenv.2009.02.038, 2009.

, Atmos. Environ., 43, 3267-3274, doi:10.1016/j.atmosenv.2009.02.038, 2009.

Lamborg, C. H., Rolfhus, K. R., Fitzgerald, W. F., and Kim, G.: The atmospheric cycling and air-sea exchange of mercury species in the South and equatorial Atlantic Ocean, Deep-Sea Res. Pt. II., 46, 957-977, doi:10.1016/s0967-0645(99)00011-9, 1999.

Landis, M. S., Stevens, R. K., Schaedlich, F., and Prestbo, E. M.: Development and characterization of an annular denuder methodology for the measurement of divalent inorganic reactive gaseous mercury in ambient air, Environ. Sci. Technol., 36, 3000-3009, doi:10.1021/es015887t, 2002.

Laurier, F. J. G., Mason, R. P., Whalin, L., and Kato, S.: Reactive gaseous mercury formation in the North Pacific Ocean's marine boundary layer: A potential role of halogen chemistry, J. Geophys. Res.-Atmos., 108, 4529, doi:10.1029/2003jd003625, 2003.

Lin, C. J., and Pehkonen, S. O.: The chemistry of atmospheric mercury: a review, Atmos. Environ., 33, 2067-2079, doi:10.1016/s1352-2310(98)00387-2, 1999.

Liu, M., Chen, L., Tao, J., Xu, Z., Zhu, L., Qian, D., and Fan, R.: Seasonal and diurnal variation of total gaseous mercury in Guangzhou City (in Chinese), China Environ. Sci., 32(9), 1554-1558, 2012.

Munthe, J., Wangberg, I., Iverfeldt, A., Lindqvist, O., Stromberg, D., Sommar, J., Gardfeldt, K., Petersen, G., Ebinghaus, R., Prestbo, E., Larjava, K., and Siemens, V.: Distribution of atmospheric mercury species in Northern Europe: final results from the MOE project, Atmos. Environ., 37, S9-S20, doi:10.1016/s1352-2310(03)00235-8, 2003.

Nakagawa, R., and Hiromoto, M.: Geographical distribution and background levels of total mercury in air in Japan and neighbouring countries, Chemosphere, 34, 801-806, doi:10.1016/s0045-6535(97)00008-8, 1997.

Nguyen, H. T., Kim, K. H., Kim, M. Y., Hong, S., Youn, Y. H., Shon, Z. H., and Lee, J. S.: Monitoring of atmospheric mercury at a global atmospheric watch (GAW) site on An-Myun Island, Korea, Water Air Soil Pollut., 185, 149-164, doi:10.1007/s11270-007-9438-5, 2007.

Nguyen, H. T., Kim, M. Y., and Kim, K. H.: The influence of long-range transport on atmospheric mercury on Jeju Island, Korea, Sci. Total Environ., 408, 1295-1307, doi:10.1016/j.scitotenv.2009.10.029, 2010.

Pan, L., Carmichael, G. R., Adhikary, B., Tang, Y., Streets, D., Woo, J.-H., Friedli, H. R., and Radke, L. F.: A regional analysis of the fate and transport of mercury in East Asia and an assessment of major uncertainties, Atmos. Environ., 42, 1144-1159, doi:10.1016/j.atmosenv.2007.10.045, 2008.

Poissant, L., Pilote, M., Beauvais, C., Constant, P., and Zhang, H. H.: A year of continuous measurements of three atmospheric mercury species (GEM, RGM and Hg-p) in southern Quebec, Canada, Atmos. Environ., 39, 1275-1287, doi:10.1016/j.atmosenv.2004.11.007, 2005.

Rutter, A. P., and Schauer, J. J.: The effect of temperature on the gas-particle partitioning of

reactive mercury in atmospheric aerosols, Atmos. Environ., 41, 8647-8657, 2007a.

Rutter, A. P., and Schauer, J. J.: The impact of aerosol composition on the particle to gas partitioning of reactive mercury, Environ. Sci. Technol., 41, 3934-3939, 2007b.

Sakata, M., and Marumoto, K.: Formation of atmospheric particulate mercury in the Tokyo metropolitan area, Atmos. Environ., 36, 239-246, doi:10.1016/s1352-2310(01)00432-0, 2002.

Sakata, M., and Marumoto, K.: Wet and dry deposition fluxes of mercury in Japan, Atmos. Environ., 39, 3139-3146, doi:10.1016/j.atmosenv.2005.01.049, 2005.

Seigneur, C. and K. Lohman.: Effect of bromine chemistry on the atmospheric mercury cycle. J. Geophys. Res., 113, D23309, doi:10.1029/2008JD010262, 2008.

Seinfeld, C. P. and Pandis, S. N.: Atmospheric Chemistry and Physics, From Air Pollution to Climate Change, 1998.

Sheu, G. R., Lin, N. H., Wang, J. L., Lee, C. T., Yang, C. F. O., and Wang, S. H.: Temporal distribution and potential sources of atmospheric mercury measured at a high-elevation background station in Taiwan, Atmos. Environ., 44, 2393-2400, doi:10.1016/j.atmosenv.2010.04.009, 2010.

Sigler, J. M., Mao, H., and Talbot, R.: Gaseous elemental and reactive mercury in Southern New Hampshire, Atmos. Chem. Phys., 9, 1929-1942, 2009.

Singh, H. B., Brune, W. H., Crawford, J. H., Flocke, F., and Jacob, D. J.: Chemistry and transport of pollution over the Gulf of Mexico and the Pacific: spring 2006 INTEX-B campaign overview and first results, Atmos. Chem. Phys., 9, 2301-2318, doi:10.5194/acp-9-2301-2009, 2009.

Slemr, F., Brunke, E. G., Ebinghaus, R., and Kuss, J.: Worldwide trend of atmospheric mercury since 1995, Atmos. Chem. Phys., 11, 4779-4787, doi:10.5194/acp-11-4779-2011, 2011.

Slinn, S.A. and W.G.N. Slinn. Predictions for particle deposition on natural waters. Atmos. Environ., 24, 1013-1016, 1980.

Soerensen, A. L., Skov, H., Jacob, D. J., Soerensen, B. T., and Johnson, M. S.: Global concentrations of gaseous elemental mercury and reactive gaseous mercury in the marine boundary layer, Environ. Sci. Technol., 44, 7425-7430, doi:10.1021/es903839n, 2010.

Stamenkovic, J., Lyman, S., and Gustin, M. S.: Seasonal and diel variation of atmospheric mercury concentrations in the Reno (Nevada, USA) airshed, Atmos. Environ., 41, 6662-6672, doi:10.1016/j.atmosenv.2007.04.015, 2007.

Steffen, A., Schroeder, W., Macdonald, R., Poissant, L., and Konoplev, A.: Mercury in the Arctic atmosphere: An analysis of eight years of measurements of GEM at Alert (Canada) and a comparison with observations at Amderma (Russia) and Kuujjuarapik (Canada), Sci. Total Environ., 342, 185-198, doi:10.1016/j.scitotenv.2004.12.048, 2005.

Temme, C., Slemr, F., Ebinghaus, R., and Einax, J. W.: Distribution of mercury over the Atlantic Ocean in 1996 and 1999-2001, Atmos. Environ., 37, 1889-1897, doi:10.1016/s1352-2310(03)00069-4, 2003.

Temme, C., Blanchard, P., Steffen, A., Banic, C., Beauchamp, S., Poissant, L., Tordon, R., and Wiens, B.: Trend, seasonal and multivariate analysis study of total gaseous mercury data from the Canadian atmospheric mercury measurement network (CAMNet), Atmos. Environ., 41, 5423-5441, doi:10.1016/j.atmosenv.2007.02.021, 2007.

Tilmes, S., Lamarque, J. F., Emmons, L. K., Conley, A., Schultz, M. G., Saunois, M., Thouret, V., Thompson, A. M., Oltmans, S. J., Johnson, B., and Tarasick, D.: Technical Note: Ozonesonde climatology between 1995 and 2011: description, evaluation and applications, Atmos. Chem.

Phys., 12, 7475-7497, doi:10.5194/acp-12-7475-2012, 2012.

Vijayaraghavan, K., P. Karamchandani, C. Seigneur, R. Balmori, and S.-Y. Chen: Plume-in-grid modeling of atmospheric mercury, J. Geophys. Res., 113, D24305, doi:10.1029/2008JD010580, 2008.

Wan, Q., Feng, X., Lu, J., Zheng, W., Song, X., Han, S., and Xu, H.: Atmospheric mercury in Changbai Mountain area, northeastern China I. The seasonal distribution pattern of total gaseous mercury and its potential sources, Environ. Res., 109, 201-206, doi:10.1016/j.envres.2008.12.001, 2009a.

Wan, Q., Feng, X., Lu, J., Zheng, W., Song, X., Li, P., Han, S., and Xu, H.: Atmospheric mercury in Changbai Mountain area, northeastern China II. The distribution of reactive gaseous mercury and particulate mercury and mercury deposition fluxes, Environ. Res., 109, 721-727, doi:10.1016/j.envres.2009.05.006, 2009b.

Wang, Y.: The speciation, levels and potential impacted factors of atmospheric mercury in Hefei, Central China (in Chinese), M.S. thesis, University of Science and Technology of China, China, 44 pp., 2010.

Wang, Z, Chen, Z, Duan, N., and Zhang, X.: Gaseous elemental mercury concentration in atmosphere at urban and remote sites in China, J. Environ. Sci.-China, 19, 176-180, doi:10.1016/s1001-0742(07)60028-x, 2007.

Wang, Z., Zhang, X., Xiao, J., Ci, Z., and Yu, P.: Mercury fluxes and pools in three subtropical forested catchments, southwest China, Environ. Pollut., 157, 801-808, doi:10.1016/j.envpol.2008.11.018, 2009.

Wang, Z., Zhang, X., Chen, Z., and Zhang, Y.: Mercury concentrations in size-fractionated airborne particles at urban and suburban sites in Beijing, China, Atmos. Environ., 40, 2194-2201, doi:10.1016/j.atmosenv.2005.12.003, 2006.

Wangberg, I., Munthe, J., Berg, T., Ebinghaus, R., Kock, H. H., Temme, C., Bieber, E., Spain, T. G., and Stolk, A.: Trends in air concentration and deposition of mercury in the coastal environment of the North Sea Area, Atmos. Environ., 41, 2612–2619, doi:10.1016/j.atmosenv.2006.11.024, 2007.

Weiss-Penzias, P., Jaffe, D. A., McClintick, A., Prestbo, E. M., and Landis, M. S.: Gaseous elemental mercury in the marine boundary layer: Evidence for rapid removal in anthropogenic pollution, Environ. Sci. Technol., 37, 3755-3763, doi:10.1021/es0341081, 2003.

Wesely, M. L.: Parameterization of surface resistances to gaseous dry deposition in regional-scale numerical models, Atmos. Environ., 23, 1293-1304, doi:http://dx.doi.org/10.1016/0004-6981(89)90153-4, 1989.

Wu, L.: Study on atmospheric mercury of Chongqing City (in Chinese), M.S. thesis, Southwest University, China, 74 pp., 2006.

Xiu, G., Cai, J., Zhang, W., Zhang, D., Bueeler, A., Lee, S., Shen, Y., Xu, L., Huang, X., and Zhang, P.: Speciated mercury in size-fractionated particles in Shanghai ambient air, Atmos. Environ., 43, 3145-3154, doi:10.1016/j.atmosenv.2008.07.044, 2009.

Yang, Y., Chen, H., and Wang, D.: Spatial and temporal distribution of gaseous elemental mercury in Chongqing, China, Environ. Monit. Assess., 156, 479-489, doi:10.1007/s10661-008-0499-8, 2009.

Yatavelli, R. L. N., Fahrni, J. K., Kim, M., Crist, K. C., Vickers, C. D., Winter, S. E., and Connell, D. P.: Mercury, PM2.5 and gaseous co-pollutants in the Ohio River Valley region: Preliminary

results from the Athens supersite, Atmos. Environ., 40, 6650-6665, doi:10.1016/j.atmosenv.2006.05.072, 2006.

Zhang, G., Zheng, X., Zhou, L., Huang, W., Qian, P., and Wang, Y.: Atmospheric mercury wet deposition and its ecological impacts in Shanghai City (in Chinese), Environ. Chem., 29(1), 147-148, 2010.

Zhang, H.: Concentrations of speciated atmospheric mercury at a high-altitude background station in the Shangri-La area of Tibetan Plateau, China, 10th International Conference on Mercury as a Global Pollutant, Halifax, Nova Scotia, Canada, 2011.

Zhang, Y., Xiu, G., Zhang, D., Zhang, M., and Zhang, R.: Total gaseous mercury in ambient air of Shanghai: its seasonal variation in relation to meteorological condition (in Chinese), Environ. Sci. Technol., 34(12), 155-158, 2012.